

# Author's Accepted Manuscript

Biomimetic magnetic sensor for electrochemical determination of scombrototoxin in fish

Amal H.A. Hassan, Luciano Sappia, Silio Lima Moura, Fatma H.M. Ali, Walaa A. Moselhy, Maria del Pilar Taboada Sotomayor, Maria Isabel Pividori



PII: S0039-9140(18)31107-X  
DOI: <https://doi.org/10.1016/j.talanta.2018.10.066>  
Reference: TAL19194

To appear in: *Talanta*

Received date: 11 July 2018  
Revised date: 15 October 2018  
Accepted date: 18 October 2018

Cite this article as: Amal H.A. Hassan, Luciano Sappia, Silio Lima Moura, Fatma H.M. Ali, Walaa A. Moselhy, Maria del Pilar Taboada Sotomayor and Maria Isabel Pividori, Biomimetic magnetic sensor for electrochemical determination of scombrototoxin in fish, *Talanta*, <https://doi.org/10.1016/j.talanta.2018.10.066>

This is a PDF file of an unedited manuscript that has been accepted for publication. As a service to our customers we are providing this early version of the manuscript. The manuscript will undergo copyediting, typesetting, and review of the resulting galley proof before it is published in its final citable form. Please note that during the production process errors may be discovered which could affect the content, and all legal disclaimers that apply to the journal pertain.

ACCEPTED MANUSCRIPT

# Biomimetic magnetic sensor for electrochemical determination of scombrototoxin in fish

Amal H.A. Hassan<sup>a,b</sup>, Luciano Sappia<sup>a</sup>, Sílvia Lima Moura<sup>a</sup>, Fatma H.M. Ali<sup>b</sup>, Walaa A. Moselhy<sup>c</sup>, Maria del  
Pilar Taboada Sotomayor<sup>d</sup>, Maria Isabel Pividori<sup>a\*</sup>

<sup>a</sup>Grup de Sensors i Biosensors, Departament de Química, Universitat Autònoma de Barcelona, Bellaterra,  
08193, Spain

<sup>b</sup>Food Hygiene and Control department, Faculty of Veterinary Medicine, Beni-Suef University, 62511  
Beni-Suef, Egypt.

<sup>c</sup>Forensic Medicine and Toxicology department, Faculty of Veterinary Medicine, Beni-Suef University,  
62511, Beni-Suef, Egypt.

<sup>d</sup>Department of Analytical Chemistry, Institute of Chemistry, State University of São Paulo (UNESP),  
14801-970 Araraquara, SP, Brazil

\*Corresponding author. María Isabel Pividori: Group de Sensors i Biosensor, Department de  
Química, Universitat Autònoma de Barcelona (UAB), 08193 Bellaterra, Barcelona, Spain. Tel.: +  
34 93 581 4937; fax:+ 34 93 581 2379. [isabel.pividori@uab.cat](mailto:isabel.pividori@uab.cat)

## Abstract

This work addresses a novel, rapid and cost-effective approach for the electrochemical sensing of scombrototoxin (histamine) in fish based on magnetic molecularly imprinted polymer (magnetic-MIP). The histamine magnetic-MIP was synthesized by the core-shell method using histamine as a template, and 2-vinyl pyridine as functional monomer. The magnetic-MIP was

ACCEPTED MANUSCRIPT

characterized by TEM, SEM, and confocal microscopy. Additionally, the binding capacity of magnetic-MIP toward histamine was investigated and compared with magnetic-NIP. This biomimetic material merged the advantages of MIPs and magnetic particles (MPs), including low cost of production, stability, high binding capacity and can be easily separated by the aid of a permanent magnet. The magnetic-MIP was integrated into magneto-actuated electrodes for the direct electrochemical detection of histamine preconcentrated from fish samples. The results revealed that this approach succeeded in the preconcentration and determination of histamine with a LOD as low as  $1.6 \times 10^{-6}$  mg L<sup>-1</sup>, much lower than index for fish spoilage (50 mg kg<sup>-1</sup>) accordingly to the legislation. Furthermore, the analytical performance was validated for the determination of histamine in scombroid fish samples with recovery values ranging from 96.8-102.0 %, confirm so it can be applied easily for routine food examination.

**Keywords:** Magnetic-MIP, scombrototoxin, histamine, electrochemical determination, fish, food safety

## 1. Introduction

Seafood, as one of the most popular and widely consumed food worldwide [1] may be a source of a lot of physical, chemical and biological hazards [2]. Biogenic amines are one of these hazards which possess a great importance in the field of food safety and quality control. They are considered indicators for early microbial decomposition of some foods. Among these biogenic amines, histamine is the most important. It plays an important role as a neurotransmitter and physiological function regulator [3]. Despite this role, it is also known as scombrototoxin as the

ingestion of histamine-rich foods causes scombroid poisoning which manifested as nausea, headache, diarrhea, and asthma [4]. Histamine is formed in a variety of L-histidine rich food e.g scombroid fish, fish products, meat, egg, cheese and fermented foods. The principal mechanism of histamine formation in foods is the enzymatic decarboxylation of free histidine by histidine decarboxylase enzyme produced by some bacteria, including *Morganella morganii*, *Klebsiella pneumoniae*, *Hafnia alvei*, *Citrobacter freundii*, and *Escherichia coli* [5]. Inappropriate handling and inadequate refrigeration favor the growth of histamine forming bacteria and lead to rapid formation of histamine in fish which rapidly increases and reaches an extremely high level within one or two days, accompanied by the apparent changes in color, odor, and texture [6,7]. Histamine is a heat stable substance once it was produced, it cannot be destroyed by heat treatment of food. As histamine content in food is considered one of the most important indicators of food quality, the United States Food and Drug Administration (FDA) has established 50 mg kg<sup>-1</sup> of histamine as the chemical index for fish spoilage [8]. Histamine can be separated and detected in complex food samples by high-performance liquid chromatography (HPLC) with fluorescence detection [9-11] and gas chromatography-mass spectrometry (GC-MS) [12]. Other detection methods involved enzymatic isotopic assay [13], and radioimmunoassay (RIA) [14]. However, these methods are expensive, laborious, time-consuming, required excessive sample pretreatment and highly qualified technicians to perform the analysis. The drawbacks of these methods in addition to the hazardous effects of histamines are imperative to find a novel, accurate and rapid method for determination of histamine in complex food samples. Molecularly imprinted polymers (MIPs) are synthetic highly cross-linked macromolecular structures towards the template, which is then extracted after polymerization, originating cavities mimicking the binding sites of the antibodies complementary in shape and size and functional groups to the template molecule [15]. These biomimetic materials are characterized by their chemical and mechanical stability, re-usability and the ability to work in harsh conditions, furthermore, they possess a great

affinity and specificity to rebind the template in a manner comparable to antibody-antigen binding [16]. Recent works reported the synthesis of molecularly imprinted polymers for the determination of histamine [17,18]. Furthermore, the electrochemical detection of this toxin was also previously reported [19, 20]. However, few of them focused on the electrochemical sensing of histamine by molecularly imprinted polymer based sensors [21]. Magnetic particles (MPs) proved its power as a preconcentration tool in a variety of analytical and biotechnology applications, e.g. PCR, immunoassays, biosensors and microfluidic devices for biomarker detection of infectious diseases [22] and foodborne pathogens [23]. The merging of the outstanding properties of MIPs and MPs to improve the washing steps and minimizing the matrix effect is a key advantage of the magnetic-MIP. Magnetic-MIP was applied in different fields for different purposes, ranging from separation [24-26], catalysis [27], and magneto immunoassays [28]. Lately, our group reported a simple method combining the isolation and preconcentration by magnetic-MIPs on m-GEC (graphite-epoxy composite magneto-actuated electrodes) of electroactive molecules for the direct electrochemical detection in complex samples [29,30]. Since the early reports on magneto-actuated electrode based on graphite epoxy composite [31,32], m-GECs were used by our research group in combination with magnetic particles as a powerful and versatile preconcentration tool in a variety of analytical and biotechnology applications. Moreover, m-GECs were previously characterized in terms of re-usability, reproducibility of the construction, and stability [33]. This work addresses the synthesis of a magnetic molecularly imprinted polymer toward histamine for the preconcentration of this biogenic amine from fish samples. The quantification of histamine was then performed by magnetic-actuation of the magnetic-MIPs for further electrochemical read-out on the surface of a magneto electrode. To the best of our knowledge, no study was reported for the integration of magnetic molecularly imprinted polymers for the direct electrochemical determination of histamine on magneto actuated electrodes.

## 2. Materials and methods

### 2.1. Chemicals

Histamine dihydrochloride, cadaverine dihydrochloride, putrescine dihydrochloride and tryptamine were purchased from Sigma Aldrich. All reagents used in the synthesis of magnetic-MIP including iron(II) chloride ( $\text{FeCl}_2 \cdot 4\text{H}_2\text{O}$ ) and iron(III) chloride ( $\text{FeCl}_3 \cdot 6\text{H}_2\text{O}$ ), ammonium hydroxide ( $\text{NH}_4\text{OH}$ ), tetraethyl orthosilicate (TEOS), 3-(trimethoxysilyl)propyl methacrylate (MPS), ethylene glycol dimethacrylate (EGDMA), 2-vinyl pyridine, methacrylic acid, toluene, ethanol, methanol, and acetic acid were analytical grade and purchased from Sigma–Aldrich. 2,2-Azobis-isobutyronitrile (AIBN) from Fisher. Unless otherwise indicated, phosphate buffer solution (PBS) was  $0.1 \text{ mol L}^{-1} \text{ Na}_2\text{HPO}_4$ ,  $0.1 \text{ mol L}^{-1} \text{ KCl}$ ,  $\text{pH}=7.0$ ). Britton-Robinson buffer (BR) was  $0.04 \text{ mol L}^{-1} \text{ H}_3\text{BO}_3$ ,  $0.04 \text{ mol L}^{-1} \text{ H}_3\text{PO}_4$  and  $0.04 \text{ mol L}^{-1} \text{ CH}_3\text{COOH}$ ,  $\text{pH}=2.0$ . Fluorescein isothiocyanate (FITC) was purchased from Sigma and the synthesis of the histamine-FITC tracer is detailed described in Supp data.

### 2.2. Instrumentation

The electrochemical measurements were performed by a CH instruments using a magneto-actuated graphite-epoxy carbon (m-GEC) [30] as working electrode (geometric area =  $0.5 \text{ cm}^2$ ), prepared as detailed shown in Figure S1 (Supp data). The characterization of the magneto electrodes (including reproducibility of the construction, renewal and reusability, and stability has been extensively reported by our research group [33]. A Ag/AgCl/KCl(satd.) reference electrode and a platinum wire as counter electrode and a standard one compartment three-electrode cell were used in all experiments. For studying the surface, The SEM images were taken with the scanning electron microscope MERLIN FE-SEM (resolution:  $0.8 \text{ nm}$  at  $15\text{kV}$ ; acceleration voltage: from  $0.2$  to  $30 \text{ kV}$ ) and SEM Hitachi S-570 (resolution:  $3.5\text{nm}$  at  $30\text{kV}$ ; acceleration voltage: from  $0.5$  to  $30 \text{ kV}$ ). E5000 Sputter Coater Polaron

ACCEPTED MANUSCRIPT  
Equipment Limited metallizer and K850 Critical Point Drier Emitech (Ashford, UK) were used for sample treatment. The TEM images were taken with the transmission electron microscope JEM-2011 (Resolution: 0.18 nm at 200 kV; acceleration voltage: 80 - 200 kV; EDS Detector Oxford LINCA) in order to determine the distribution, size and shape of the magnetic-MIP particles. The confocal fluorescence images were taken with the TCP-SP5 Leica Microscope, being the images processed with the Imaris X64 v.6.2.0 software (Bitplane, Switzerland). Ultra violet absorption spectra were recorded by a UVR spectrophotometer (*hp* 8453). Magnetic separation during the washing steps was performed by a magnetic separator Dynal MPC-S (Product N 120.20D, Dynal Biotech ASA, Norway).

### 2.3. Computer simulation for the rational design of the magnetic molecularly imprinted polymer for histamine

In order to select the monomer for the synthesis of the magnetic-MIP among different candidates, an *in silico* simulation was performed by molecular mechanics using a desktop PC running Microsoft Windows XP Professional operating system. The functional monomer for the synthesis of imprinted polymer was selected from molecular modeling studies, using computer programs HyperChem 8.0.5 (Hypercube, Inc., Gainesville, Florida, USA) and OpenEye (OpenEye scientific software, Inc., Santa Fe, New Mexico, USA). More details are provided in Supp. data.

### 2.4 Synthesis of the magnetic-MIPs for histamine

The synthesis of magnetic-MIP was performed by core shell method following the protocol of our research group [31], with some modifications. The experimental details are provided in Supp. data and schematically shown in Figure S2. Briefly, the synthesis of the Fe<sub>3</sub>O<sub>4</sub> magnetic core was performed by co-precipitation of a Fe<sup>2+</sup>/Fe<sup>3+</sup> mixed solution. Then, the Fe<sub>3</sub>O<sub>4</sub> nanoparticles were modified with tetraethyl orthosilicate (TEOS) to provide OH groups for further reaction.

After that, the hydroxyl modified magnetic particles ( $\text{Fe}_3\text{O}_4@\text{SiO}_2$ ) was reacted with the acrylic group of 3-methacryloxypropyltrimethyloxysilane (MPS), to provide activated C=C groups for further co-polymerization. The pre-polymerization mixture was performed by mixing the monomer 2-vinyl pyridine and the template histamine. The  $\text{Fe}_3\text{O}_4@\text{SiO}_2$ -MPS were added to the pre-polymerization mixture with the crosslinking monomer, (ethylene glycol dimetacrylate, EGDMA) and the radical initiator, (azobisisobutyronitrile, AIBN) using toluene as a porogenic solvent. Finally, the washing step was performed using a soxhlet extraction and methanol:acetic acid 9:1 as extracting solvent in order to extract histamine from magnetic-MIP. The solution was changed every 12 hours during five days. After that the product was dried at RT. Similarly, the magnetic non-molecularly imprinted polymers (magnetic-NIPs) were prepared with the absence of the template.

## 2.5. Characterization of the magnetic-MIP

### 2.5.1. Scanning electron microscopy (SEM) and Transmission electron microscopy (TEM)

After each step of the synthesis, a small amount of the product was collected and prepared for SEM and TEM as detailed in Supp data. Energy dispersive X-ray spectroscopy detector (EDS) was also used for the elemental analysis.

### 2.5.2. Confocal microscopy study

Confocal fluorescence microscopy was performed to evaluate the binding performance of the magnetic-MIP to capture and preconcentrate histamine. The histamine FITC tracer solution was incubated with magnetic-MIP or magnetic-NIP ( $5.0 \text{ mg mL}^{-1}$ ) for 1h at RT with agitation at 750 rpm (2 RCF). Samples were then washed three times with PBS and examined by confocal microscopy with the laser lines of 492 nm excitation and 518 nm emission. Other characterization of the material during the synthesis was performed, including selected-area diffraction analysis (SAED), X-ray diffraction, UV spectrophotometry.



## 2.6. Binding study

The binding experiments were performed by adding 5.0 mg of magnetic-MIP and magnetic-NIP as a control to 1.0 mL of different concentrations of histamine ranged from 0 to 111 mg L<sup>-1</sup> at RT in PBS. The mixture was shaken in a rotary shaker at 750 rpm (2 RCF). for 60 min. The magnetic polymer suspensions were separated by external neodymium magnetic bar. The absorbance of the supernatant was measured at a wavelength of 210 nm. The amount of histamine adsorbed by magnetic-MIP ( $Q_e$ , mg g<sup>-1</sup>) was calculated as follow:

$$Q_e = \frac{V(C_0 - C_e)}{m} \quad (\text{Eq. 1})$$

Where  $Q_e$  (mg g<sup>-1</sup>) is the experimental equilibrium adsorption capacity,  $C_0$  (mg L<sup>-1</sup>) is the initial concentration of histamine,  $C_e$  (mg L<sup>-1</sup>) is the equilibrium concentration of histamine dihydrochloride,  $V$  (mL) is the volume of the solution and  $m$  (mg) is the weight of magnetic-MIP or magnetic-NIP.

Setting the binding experiment parameters has a great influence on the results of binding capacity. Therefore, the effect of binding time was determined by mixing 5.0 mg of magnetic-MIP with 1.0 mL of 55.6 mg L<sup>-1</sup> histamine solution and incubated by changing the binding time from 0 to 60 minutes. The magnetic polymer suspensions were separated by external neodymium magnetic bar. The absorbance of the supernatant was measured at 210 nm. For investigating the effect of the magnetic polymers amount on the adsorption capacity, different amount of magnetic-MIP and magnetic-NIP as a control ranged from 1.0 to 10.0 mg were mixed with 1.0 mL histamine solution (55.6 mg L<sup>-1</sup>) and shaken in a rotary shaker at 750 rpm (2 RCF) for 60 min. The magnetic polymer suspensions were separated by external neodymium magnetic bar. The solution was measured by ultraviolet visible spectrophotometer at a wavelength of 210 nm.

## 2.7. Electrochemical sensing of scombrotoxin on m-GEC electrode by preconcentration on magnetic-MIP

As schematically shown in Fig.1, the direct electrochemical determination of histamine was carried out by preconcentration on the magnetic-MIP with further magnetic actuation on the surface of m-GEC electrode. The cyclic voltammetry was investigated on m-GEC electrode in 20 mL PBS containing  $111.0 \text{ mg L}^{-1}$  histamine solution at a scan rate of  $0.05 \text{ Vs}^{-1}$  between  $-0.2$  to  $1.6 \text{ V}$ . Furthermore, the electrochemical behavior of histamine was examined on different supporting electrolyte solution including PBS and BR buffer. The effect of scan rate ranged from  $0.03$  to  $0.15 \text{ Vs}^{-1}$  on the oxidation current and potential was studied. Furthermore, the effect of the pH for PBS in the range of 5 to 9 on the peak current and potentials of  $111.0 \text{ mg L}^{-1}$  histamine was investigated.

After setting all the parameters, the direct electrochemical detection of histamine (without preconcentration on magnetic-MIP) was performed on bare m-GEC electrodes by CV at a scan rate of  $0.05 \text{ Vs}^{-1}$  between  $-0.2$  to  $1.6 \text{ V}$  vs AgCl/KCl (satd.) reference electrode by spiking  $100 \text{ }\mu\text{L}$  histamine (ranging from 0 to  $2.2 \times 10^4 \text{ mg L}^{-1}$ ) in  $20.0 \text{ mL}$  of PBS ( $0.1 \text{ mol L}^{-1} \text{ Na}_2\text{HPO}_4$ ,  $0.1 \text{ mol L}^{-1} \text{ KCl}$ ,  $\text{pH}=7.0$ ).

Finally, the detection of histamine preconcentrated on magnetic-MIP by magnetic actuation on m-GEC electrode was performed [29]. To achieve that, the magnetic-MIPs ( $100 \text{ }\mu\text{L}$  at  $5.0 \text{ mg mL}^{-1}$ ) was incubated with  $100 \text{ }\mu\text{L}$  histamine ranging from 0 to  $11.1 \text{ mg L}^{-1}$  in PBS for 60 min with gently shaking at RT. The magnetic-MIP with the preconcentrated histamine was then magneto-actuated on the surface of the m-GEC electrode by simply dipping the magnetic electrode in the incubation tube for capturing the magnetic-MIP [29]. The electrochemical readout was the performed by cyclic voltammetry (CV) at a scan rate of  $0.05 \text{ Vs}^{-1}$  between  $-0.2$  to

1.6 V vs AgCl/KCl(satd.) reference electrode. As a negative control, the magnetic-NIP was processed in the same way.

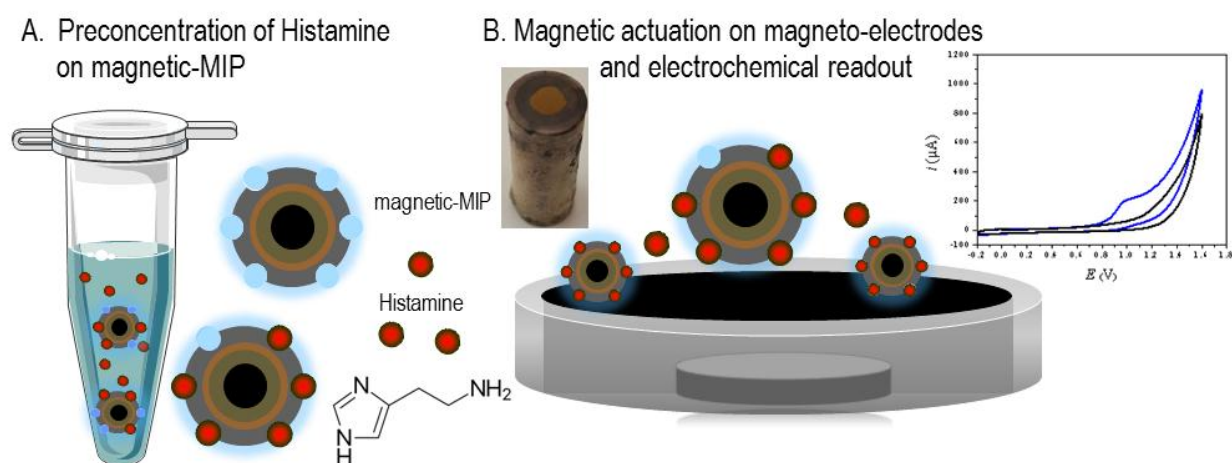


**Fig. 1.** Schematic procedure for the electrochemical sensing of histamine preconcentrated on magnetic-MIP by magnetic actuation on m-GEC electrodes.

## 2.8. Study of interferences

This experiment was carried out to investigate the effect of presence of some interferences similar or related to histamine on the selectivity of magnetic-MIP. This was achieved by mixing 100.0  $\mu\text{L}$  of magnetic-MIP with 100  $\mu\text{L}$  of 0.111  $\text{mg L}^{-1}$  of histamine in the presence of some other biogenic amines including cadaverine, putrescine, tryptamine) for 60 minutes under stirring then the magnetic-MIP with the preconcentrated histamine was magneto actuated on m-GEC electrode and the oxidation current response was measured in 20.0 mL of PBS at a scan rate of 0.05  $\text{Vs}^{-1}$  between -0.2 to 1.6 V vs AgCl/KCl (satd.) reference electrode.

## 2.9. Electrochemical sensing of scombrototoxin in fish samples

Histamine is an important indicator for early food decomposition and the ingestion of food containing histamine causes what is called scombroid food poisoning in man, so the monitoring of its contents in food is an essential issue. Scombroid fish (e.g. *Thunnus albacares* commonly known

as tuna) despite its popularity and highly consumption, is highly and the firstly incriminated in scombroid food poisoning, so it must be efficiently examined. A simple and efficient method for extraction of histamine from fish samples was applied as follow. Briefly, tuna fish samples were purchased from fish market retail store in Barcelona and homogenized by food blender. Samples were spiked with histamine at different concentrations levels, ranging from 0 to 3 mg kg<sup>-1</sup>. The spiked fish samples were mixed with PBS, mechanically stirred, then ultrasonicated for 10 min. The resulted mixture was centrifuged and filtered. The filtrate (100 μL) was mixed with 100 μL magnetic-MIP (5 mg mL<sup>-1</sup>) and left to bind for 60 min under shaking at room temperature. The magnetic polymer suspensions were separated by external neodymium magnetic bar, then the magnetic-MIP with the preconcentrated histamine dihydrochloride was magneto-actuated on m-GEC electrode and the anodic current response was measured in 20.0 mL of PBS at a scan rate of 0.05 Vs<sup>-1</sup> between -0.2 to 1.6 V vs AgCl/KCl(satd.) reference electrode.

### 3. Results and discussion

#### 3.1. Computer simulation for the rational design of magnetic molecularly imprinted polymer for histamine

The theoretical study is presented in Supp. Data. According to the theoretical results (Fig. S3), 2-vinyl pyridine was considered to be a suitable monomer for MIP design for histamine among the studied 20 monomers (Table S1). The 2-vinyl pyridine–histamine complex presents the stronger interactions due to possessing the higher binding energy. Regarding to the theoretical results, this work focused on using 2-vinyl pyridine as a functional monomer for the synthesis of magnetic-MIP for histamine. The effect of the solvent was also considered in Supp. data.

#### 3.2. Synthesis and characterization of the magnetic-MIP

The synthesis of magnetic-MIP toward histamine as illustrated in Fig. S2 was detailed in the Supp. data (Schemes S1–S3). Along the synthesis procedure the product of each step was collected for further characterization.

In order to elucidate the crystal structure of the material, the magnetic core of  $\text{Fe}_3\text{O}_4$  nanoparticles were evaluated by selected-area electron diffraction (Fig. S4 and Table S2), and by X-ray diffraction (Fig. S5, Supp. data). X-ray diffraction (XRD) of the  $\text{Fe}_3\text{O}_4$  nanoparticles revealed six characteristic peaks located at  $2\theta$  of  $30.36^\circ$ ,  $35.61^\circ$ ,  $43.47^\circ$ ,  $53.56^\circ$ ,  $57.10^\circ$  and  $62.75^\circ$  corresponding to  $\text{Fe}_3\text{O}_4$  in the material (Fig. S5). The diffractograms of samples showed the planes (220, 311, 400, 422, 511 and 440) corresponding to a pure cubic spinel crystal structure of  $\text{Fe}_3\text{O}_4$  [32].

The scanning electron microscopy provides great details about the polymers morphology along each step of the synthesis. The magnetic nanoparticles are completely coated with TEOS and MPS (Fig. S6, panel B,C) and retaining their spherical like shape. These spherical like particles tend to agglomerate in case of magnetic-MIP (Fig. S6, panel D).

The results of macroscopic images, TEM and elemental analysis by Energy dispersive X-ray spectroscopy are presented in Fig. S7 (Supp. data). As observed, the size of the particles increased with each step of the core-shell synthesis due to the layer by layer added to the outer part of the magnetic core of the nanoparticles to be spherical in shape and more aggregated (Fig. S7). The average particle diameter ranges from 15 nm (SD 2) for the magnetite core of  $\text{Fe}_3\text{O}_4$ , to 77 nm (SD 18) for the first layer ( $\text{Fe}_3\text{O}_4@ \text{SiO}_2$ ) and 179 nm (SD 23) for the second layer ( $\text{Fe}_3\text{O}_4@ \text{SiO}_2\text{-MPS}$ ). From the TEM imaged it can be concluded that the size of the magnetic-NIP and MIP increases, but it was not possible to determine the diameter on a representative number of entities due to the aggregation and the superposition of the different polymerization layers. The aspect of magnetic-MIP and magnetic-NIP are comparatively shown in detail in Fig. 2. It can be noticed the differences in the porosity pattern of the magnetic-MIP

(panel A) compared to the magnetic-NIP (panel B), which can be attributed to the cavities after histamine extraction. Furthermore, as also confirmed by SEM (Figure S6), the Figure 2 revealed irregular spherical shape nanoparticles highly cross-linked among them containing many nanoparticles of magnetite in the structure.

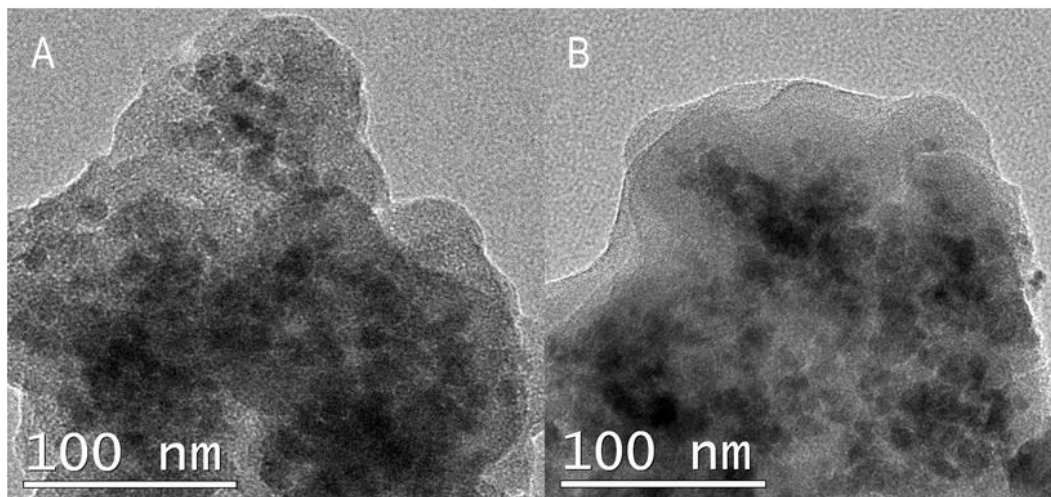


**Fig. 2.** Comparative study of magnetic-MIP (Panel A) and magnetic-NIP (Panel B) by transmission electron microscopy.

Further characterization was performed by using confocal microscopy. Fig.3 shows the higher binding capacity of the magnetic-MIP to the histamine-FITC tracer, as compared with magnetic-NIP. In case of magnetic-NIP, small fluorescence is also observed which can be attributed to non-specific adsorption of the dye due to the porosity of the polymer. Moreover, Fig.3 also compared the binding performance of the magnetic-MIP synthesized with different monomers including 2-vinyl pyridine and methacrylic acid. The fluorescence is much higher for the selected monomer highlighting the high predictive value of the theoretical results by computer simulation which suggested that the 2-vinyl pyridine is the optimal monomer for histamine magnetic-MIP synthesis.

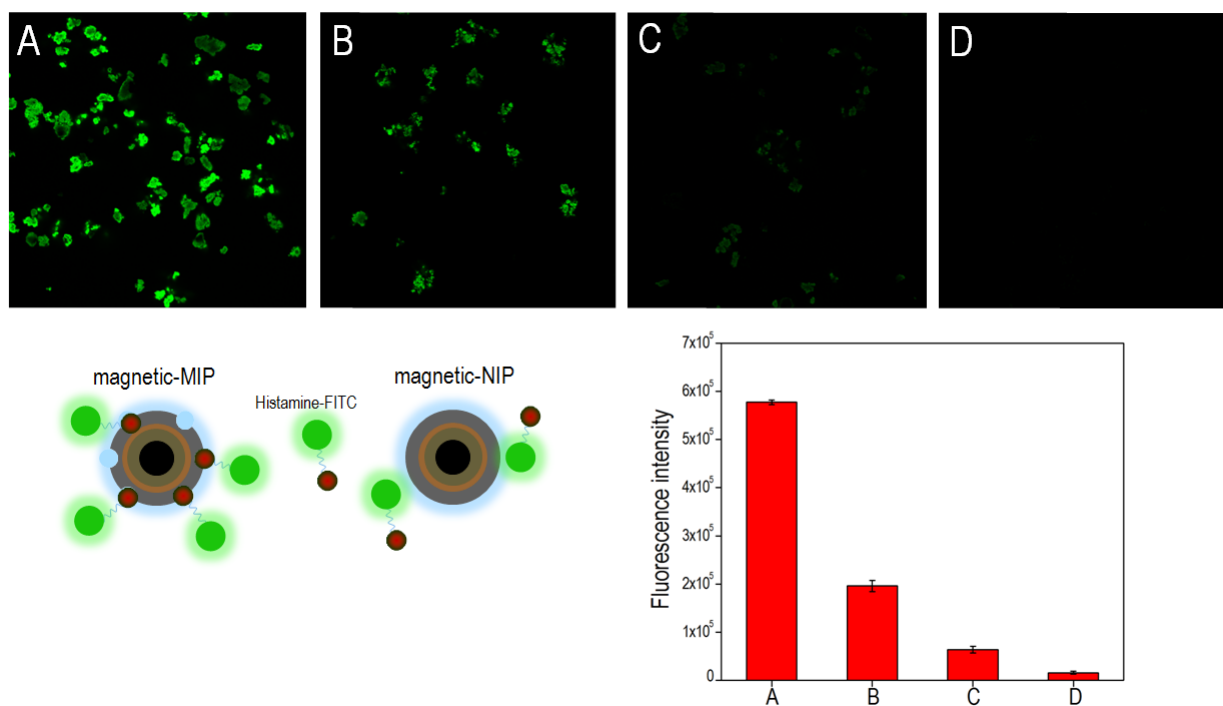


**Fig. 3.** Confocal microscopy for the characterization of the binding of histamine-FITC conjugate on 2-vinyl pyridine magnetic-MIP (A) and the corresponding NIP (B). Furthermore, the confocal images for methacrylic acid magnetic-MIP (C) and NIP (D) is also shown. The corresponding fluorescence intensity values at 518 nm for each of the material are also shown (n=3).

### 3.3. Binding study

The adsorption parameters including the binding time and the magnetic-MIP amount must be carefully studied as it gives a valuable idea about the adsorption process. Fig. S9, panel A shows the effect of binding time ranging from 0 to 60 min on the binding capacity of histamine magnetic-MIP. The binding capacity increased as the binding time increase. In order to ensure the maximum absorption from complex samples, 60 min was selected for further studies. The influence of the amount of magnetic-MIP on the binding capacity (Fig. S9, panel B), showed that the adsorption capacity increased with increasing the amount of polymer, and 5.0 mg mL<sup>-1</sup> magnetic-MIP was used for further experiments.

The kinetics adsorption for histamine at different concentration (0 to 111.0 mg L<sup>-1</sup>) on magnetic-MIP and magnetic-NIP (as a control) is illustrated in Fig. 4, panel A. The adsorption

capacity of magnetic-MIP for histamine increased while increasing its concentration, as expected. At histamine concentration up to  $111.0 \text{ mg L}^{-1}$ , the  $Q_e$  of magnetic-MIP and magnetic-NIP was about  $6.4$  and  $1.1 \text{ mg g}^{-1}$ , respectively. The maximum adsorption ratio of magnetic-MIP/magnetic-NIP was thus  $5.8$ , highlighting the selectivity of the magnetic-MIP toward histamine, which can be attributed to the presence of specific binding sites on the magnetic-MIP. This result was reinforced by the mathematical adjustment of the isotherm experimental data by the Langmuir-Freundlich model ( $R = 0.9932$ ), which allowed to estimate a value of the binding constant for the magnetic-MIP towards histamine of  $2.3 \times 10^5 \text{ L mol}^{-1}$ , indicating the high efficiency to bind the template of the synthesized magnetic-MIP based on 2-vinyl pyridine. Fig. 4, panel B shows comparatively the binding capacity of magnetic-MIP and magnetic-NIP synthesized by using 2-vinyl pyridine and methacrylic acid as monomers. Again, As in the case of the confocal microscopy study, the binding capacity of the magnetic-MIP based on 2-vinyl pyridine was much higher than for methacrylic acid, highlighting the role of the theoretical simulation to predict the monomer of choice for the synthesis of histamine magnetic-MIP.

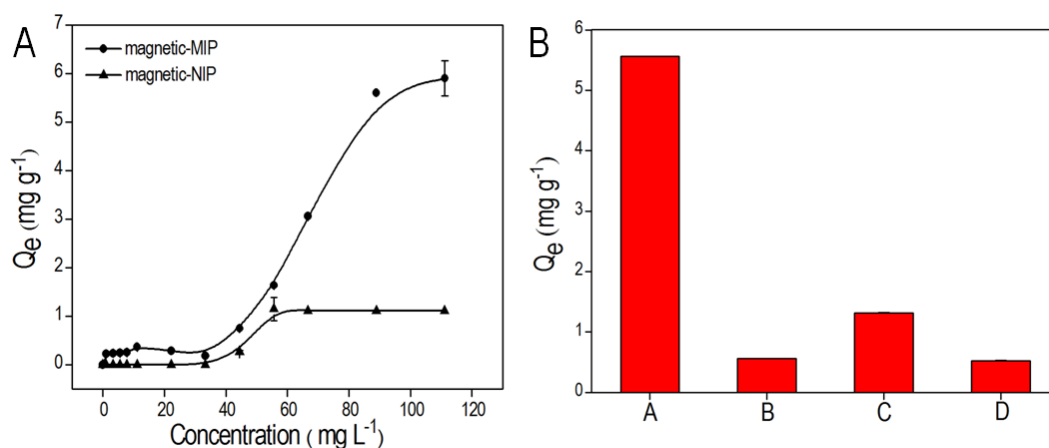




**Fig. 4.** Panel A. Binding isotherm of magnetic-MIP and magnetic-NIP ( $5.0 \text{ mg mL}^{-1}$ ) for histamine at different concentrations ( $0\text{-}111.0 \text{ mg L}^{-1}$ ) in PBS, and at a binding time of 60 min. Panel B. Comparative study of the binding capacity for  $88.9 \text{ mg L}^{-1}$  histamine in PBS of 2-vinyl pyridine magnetic-MIP (A) and the corresponding NIP (B). Furthermore, the values for methacrylic acid magnetic-MIP (C) and NIP (D) are also shown. Error bar illustrates the standard deviation ( $n=3$ ).

### 3.4. Electrochemical sensing of scombrototoxin on m-GEC electrode by preconcentration on magnetic-MIP

Firstly, the electrochemical characterization of histamine at m-GEC electrode was performed by cyclic voltammogram, as detailed in Fig. S10. A single oxidation peak was observed at  $1.04 \text{ V}$  with no corresponding reduction signal in the reverse potential scan which indicates the irreversible charge transfer of the electrode, as previously reported [19,20]. Moreover, the electrochemical characterization of histamine was examined on different supporting electrolyte solution including PBS and BR buffer.

The results in Fig. S11 showed that BR buffer solution provided a low, undefined current peak with higher background. On the other hand, a well-defined higher peak current accompanied with low background response was provided with PBS, in accordance with previous studies<sup>20</sup>[20]. Accordingly, PBS ( $0.1 \text{ mol L}^{-1} \text{ Na}_2\text{HPO}_4$ ,  $0.1 \text{ mol L}^{-1} \text{ KCl}$ ,  $\text{pH}=7.0$ ) was selected for the electrochemical determination of histamine. The optimization of scan rate was also performed as detailed in Supp data. The peak current of histamine increases as the scan rate increase and the potential peak was shifted positively (Fig. S12). Furthermore, the effect of PBS ( $0.1 \text{ mol L}^{-1} \text{ Na}_2\text{HPO}_4$ ,  $0.1 \text{ mol L}^{-1} \text{ KCl}$ ) at different pH values (ranging from  $\text{pH}=5$  to  $9$ ) were studied in Fig. S13 and the maximum electrochemical response was obtained in PBS at  $\text{pH}=7$  so it was used for further experiments. More details are provided in Supp data.

The oxidation responses of different concentrations of histamine on m-GEC electrodes (without preconcentration on magnetic-MIP) were investigated by spiking  $100 \mu\text{L}$  histamine (ranging from  $0$

to  $2.2 \times 10^4 \text{ mg L}^{-1}$  in 20.0 mL of PBS (Fig. 5, panel A). The maximal oxidation peak current was fitted by a nonlinear regression (Two site binding/hyperbola) ( $R^2 = 0.994$ ) (Figure 5, panel B).

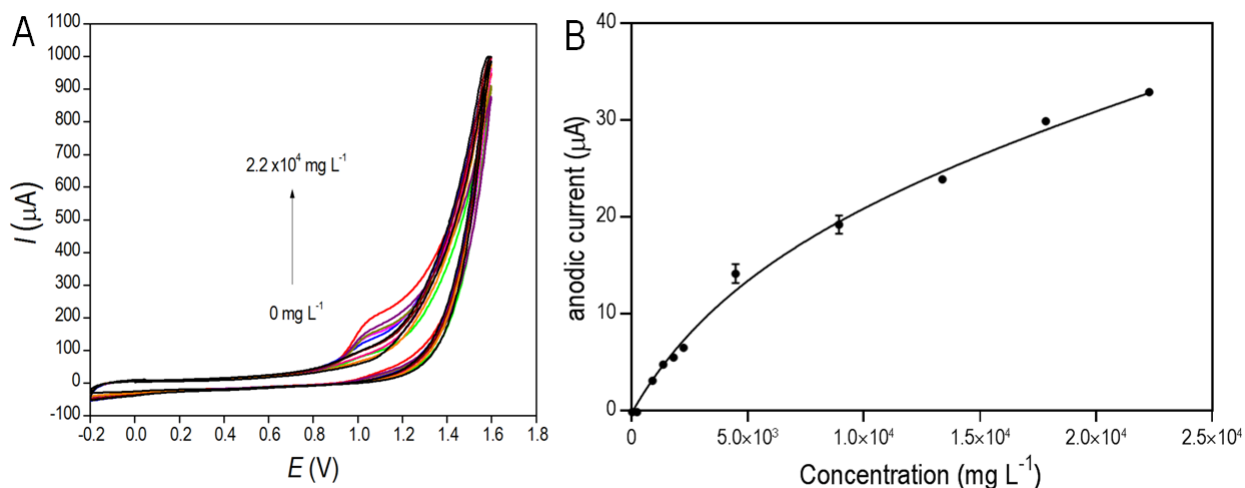


**Fig. 5.** Panel A. CV at different concentrations of histamine (ranging from 0 to  $2.2 \times 10^4 \text{ mg L}^{-1}$ ) on a bare m-GEC electrodes, and performed by spiking 100  $\mu\text{L}$  in 20 mL of PBS. Panel B. Calibration plot of the anodic current values at different concentrations of histamine ( $0\text{--}11.1 \text{ mg L}^{-1}$ ) on a bare m-GEC electrode in 20.0 mL of PBS. The oxidation peak current was fitted by a nonlinear regression (Two site binding hyperbola,  $R^2 = 0.9940$ ). Error bar shows the standard deviation ( $n=3$ ).

The LOD for the detection of histamine on the bare m-GEC electrode was thus calculated. To achieve that, the negative control samples ( $n=5$ ) were considered, obtaining a mean value of  $1.6 \mu\text{A}/\text{SD } 0.1 \mu\text{A}$ . The cut-off value was then determined with a one-tailed t-test at a 95% confidence level, giving a value of  $1.8 \mu\text{A}$  ( $t_{0.050}=2.132$ ,  $n=5$ ). This value was interpolated in the calibration plot showed in Figure 5, panel B, and the LOD was found to be as low  $2.2 \text{ mg L}^{-1}$  in the electrochemical cell, corresponding to  $453.0 \text{ mg L}^{-1}$  (in 100  $\mu\text{L}$  sample).

For electrochemical sensing of histamine preconcentrated on the magnetic-MIP, 100  $\mu\text{L}$  of histamine ranging from 0 to  $11.1 \text{ mg L}^{-1}$  was preconcentrated on the magnetic-MIP for 60 min and then the magnetic-MIP was magneto actuated on m-GEC electrode and the oxidation current was

investigated by CV (Fig. 6 panel A). The maximal oxidation peak current was fitted by a nonlinear regression (Two site binding hyperbola,  $R^2 = 0.9083$ ) (Figure 6, panel A). The LOD for the detection of histamine preconcentrated on the magnetic-MIP was thus calculated, by processing the negative control samples ( $n=6$ ), obtaining a mean value of  $1.5 \mu\text{A}/\text{SD } 0.3 \mu\text{A}$ . The cut-off value was then determined with a one-tailed t-test at a 95% confidence level, giving a value of  $2.0 \mu\text{A}$  ( $t_{0.050}=2.015$ ,  $n=6$ ). This value was interpolated and the LOD was found to be as low as  $1.6 \times 10^{-6} \text{ mg L}^{-1}$  much lower than the permissible limit in fish. This value is also lower than the previously reported work for electrochemical determination of histamine<sup>192021</sup> [19-21]. This could be attributed to the ability of magnetic-MIP to bind and preconcentrate histamine on the surface of m-GEC

Figure 6, panel A also shown the direct anodic signals for histamine determined by the bare m-GEC electrode (without preconcentration) at the same concentration range, highlighting the outstanding capacity of the magnetic-MIP to preconcentrated histamine and thus to improve the LOD in the original  $100 \mu\text{L}$  sample from  $453.0 \text{ mg L}^{-1}$  (as calculated in the bare m-GEC electrode) to as low as  $1.6 \times 10^{-6} \text{ mg L}^{-1}$  by preconcentration of the magnetic-MIP.

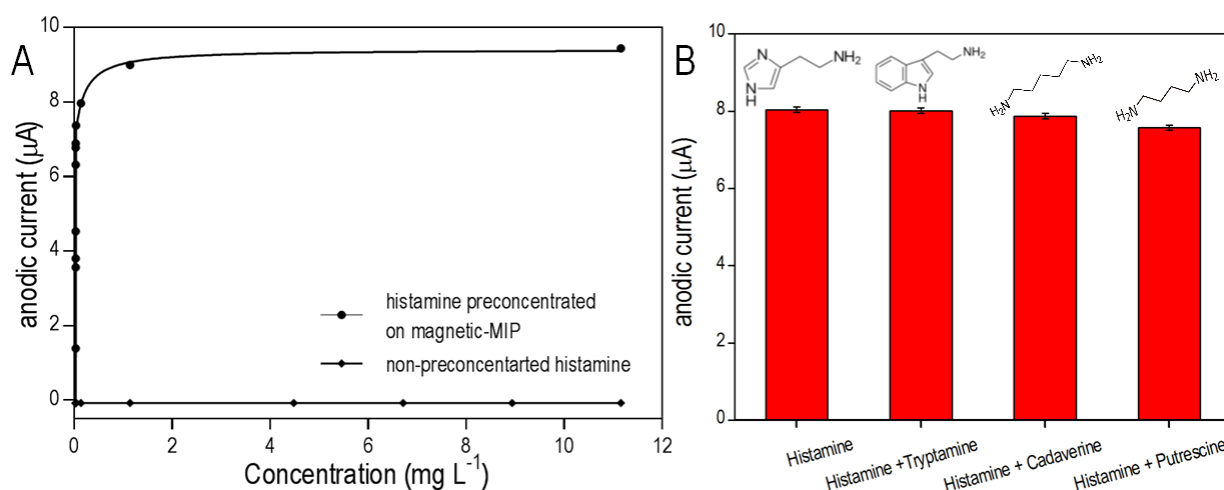


**Fig. 6.** Panel A. Calibration plot of the anodic current values at different concentrations of histamine ( $0-11.1 \text{ mg L}^{-1}$ ) with and without preconcentration on the magnetic-MIP and examined by

CV at m-GEC in 20.0 mL of PBS. The oxidation peak current was fitted by a nonlinear regression (Two site binding hyperbola,  $R^2 = 0.9083$ ). Panel B. Study of the selectivity of the magnetic-MIP toward histamine. Histamine was preconcentrated on magnetic-MIP in the presence of biogenic amines and examined by CV at m-GEC in 20.0 mL of PBS. Error bar illustrates the standard deviation (n=3).

### 3.5. Study of interferences

Fig. 6 panel B also showed the effect of the presence of some biogenic amines on the selectivity of magnetic-MIP towards histamine by electrochemical examination by CV on m-GEC. As shown, the present of foreign substances or interference was found to be negligible, highlighting the specificity of the magnetic-MIP towards histamine. The results were statistically analyzed by one way ANOVA ( $p > 0.01$ ) revealing that there is no significance difference between the oxidation current response induced by histamine preconcentrated on magnetic-MIP either alone or in the presence of interferences.

### 3.6. Electrochemical sensing of scombrototoxin in fish samples

Table 1 shows the recovery values for histamine in fish samples (tuna) from local retail markets performed by preconcentration on the magnetic-MIPs, magnetic actuation on m-GEC electrodes, and electrochemical sensing by CV. The average recoveries ranged between 96.8 % and 102.0 %. This satisfactory recovery rate proves that the synthesized magnetic-MIP keeps the affinity towards the template even in complex samples, and can be applied for rapid determination of histamine in complex food samples. Because of the complexity of fish as a food matrix, this technique could be also applied for the determination of histamine in other kinds of L-histidine rich foods.

**Table 1.** Recovery (mean value/SD, for n = 3) for the determination of histamine in fish samples

<b>Histamine spiked</b> <b>(mg kg<sup>-1</sup>)</b>	<b>Histamine detected</b> <b>(mg kg<sup>-1</sup>) mean/SD</b>	<b>RSD %</b>	<b>Recovery %</b>
0.00	0.00	0.0	0.0
0.60	0.62/0.02	3.2	102.0
1.80	1.780/0.005	0.3	98.4
3.00	2.92/0.03	1.2	96.8

## Conclusion

In summary, a sensitive and rapid method for the electrochemical determination of histamine in fish samples based on magnetic-MIP for preconcentration and selective binding is described. The magnetic-MIP showed a high binding capacity towards histamine as compared with the corresponding magnetic-NIP. The electrochemical sensor based on magnetic-MIP offer an exciting alternative by replacing the current methods for detection of histamine due to the analytical features, including assay time (60 min), simplicity, long-term storage, LOD (as low as  $1.6 \times 10^{-6}$  mg L<sup>-1</sup>, much lower than the permissible limit in fish), low cost and animal-free production of reagents. This novel material succeeded in the preconcentration of histamine from fish samples with a recovery rate ranged between 96.8-102.0 %. These good results prove the ability of this material to preconcentrate histamine from complex food samples as fish, even in the presence of other biogenic amines, including cadaverine, putrescine and tryptamine. It is important to highlight the outstanding LOD provided by this approach compared with other reported electrochemical biosensors (Table S3) due to the ability of the magnetic-MIP for the specific preconcentration of histamine. Furthermore, this approach shows promising features to

be used in different food items as future perspectives of this work. This simple and rapid technology will open the way to incorporate this material in different magneto actuated device could be used easily in the field of food safety and environmental monitoring with no need to extensive sample pretreatment and sophisticated instruments.

### **Acknowledgement**

Financial support from the Ministry of Economy and Competitiveness (MINECO), Madrid (Grants BIO2013-41242-R and BIO2016-75751-R) are gratefully acknowledged. Egyptian Government is gratefully acknowledged for her assistance.

### **Appendix A. Supplementary data**

### **Competing of interests**

The authors have no competing of interests.

### **References**

- [1] OECD/FAO (2016), OECD-FAO Agricultural Outlook 2016-2025, OECD Publishing, Paris.
- [2] P. Visciano, M. Schirone, R. Tofalo, G. Suzzi, Biogenic Amines in Raw and Processed Seafood, *Front Microbiol.* 3 (2012) 188.
- [3] M. Jutel , T. Watanabe , M. Akdis, K. Blaser , C.A. Akdis, Immune regulation by histamine, *Curr. Opin. Immunol.* 14 (2002) 735–740.
- [4] S.L. Taylor, R.R. Eitenmiller, Histamine food poisoning: toxicology and clinical aspects, *CRC Crit. Rev. Toxicol.* 17 (1986) 91-128.
- [5] S.L. Taylor, M.W. Speckhard, Isolation of histamine-producing bacteria from frozen tuna, *Mar. Fish. Rev.* 45 (1983) 6.

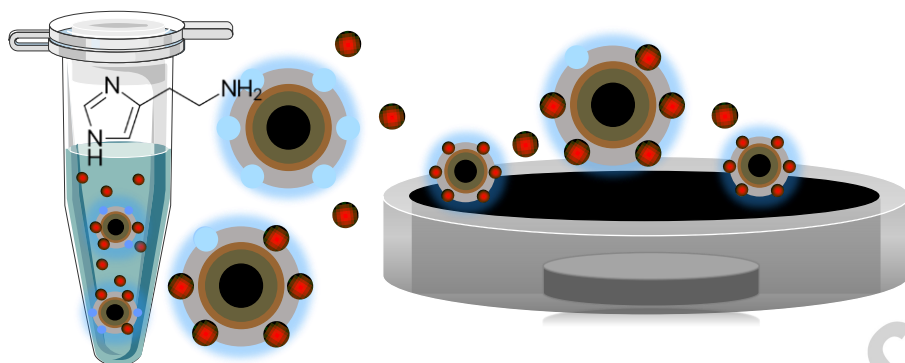
- [6] N. Guizani, M.A. Al-Busaidy, I.M. Al-Belushi, A. Mothershaw, M.S. Rahman, The effect of storage temperature on histamine production and the freshness of yellow fin tuna (*Thunnus albacares*), *Food Res. Int.* 38 (2005) 215-222.
- [7] C.C. Silva, D.J. Ponte, M.L.E. Dapkevicius, Storage temperature effect on histamine formation in big eye tuna and skipjack, *J. Food Sci.* 63 (1998) 644-647.
- [8] Department of Health and human Services, Public Health service, Food and Drug Administration, Center for Food Safety and Nutrition, Fish and Fishery products Hazards and Controls Guidance, 4th ed., 2011, April.
- [9] Y. Miyamoto, R. Yoshimoto, M. Yumoto, A. Ishihara, K. Takahashi, H. Kotani, A. Kantani, S. Tokita, Simultaneous fluorometric measurement of histamine and N-methyl histamine levels in rodent brain by high-performance liquid chromatography, *Anal. Biochem.* 334 (2004) 89–96.
- [10] Y. Tsuruta, K. Kohashi, Y. Ohkura, Simultaneous determination of histamine and N-methyl histamine in human urine and rat brain by high-performance liquid chromatography with fluorescence detection, *J. Chromatogr.* 224 (1981) 105–110.
- [11] A. Yamatodani, H. Fukuda, H. Wada, T. Iwaeda, T. Watanabe, High-performance liquid chromatographic determination of plasma and brain histamine without previous purification of biological samples: cation-exchange chromatography coupled with post-column derivatization fluorometry, *J. Chromatogr.* 344 (1985) 115–123.
- [12] J.J. Keyzer, B.G. Wolthers, F.A. Muskiet, H. Breukelman, H.F. Kauffman, K. de Vries, Measurement of plasma histamine by stable isotope dilution gas chromatography–mass spectrometry: methodology and normal values, *Anal. Biochem.* 139 (1984) 474–481.
- [13] M.A. Beaven, S. Jacobsen, Z. Horakova, Modification of the enzymatic isotopic assay of histamine and its application to measurement of histamine in tissues, serum, and urine, *Clin. Chim. Acta.* 37 (1972) 91–103.

- [14] E. Hammar, A. Berglund, A. Heiden, A. Norrman, K. Rustas, U. Ytterström, E. Akerblom, An immunoassay for histamine based on monoclonal antibodies, *J. Immunol. Methods*. 128 (1990) 51–58.
- [15] K. Haupt, Biomaterials: Plastic antibodies, *Nature Mater.* 9 (2010) 612-614.
- [16] L. Ye, K. Haup, Molecularly imprinted polymers as antibody and receptor mimics for assays, sensors and drug discovery, *Anal. Bioanal. Chem.* 378 (2004) 1887–1897.
- [17] F. Gao, E. Grant, X. Lu, Determination of histamine in canned tuna by molecularly imprinted polymers-surface enhanced Raman spectroscopy, *Anal. Chim. Acta.* 901 (2015) 68-75.
- [18] F.A. Trika, K. Yoshimatsu, L. Ye, D.A. Kyriakidis, Molecularly imprinted polymers for histamine recognition in aqueous environment, *Amino Acids*. 43 (2012) 2113-2124.
- [19] A. Geto, M. Tessema, S. Admassie, Determination of histamine in fish muscle at multi-walled carbon nanotubes coated conducting polymer modified glassy carbon electrode, *Synth. Met.* 191 (2014) 135-140.
- [20] Z.S. Stojanovic, E. Mehmeti, K. Kalcher, V. Guzsanyi, SWCNT- modified carbon paste electrode as an electrochemical sensor for histamine determination in alcoholic beverages, *Food Anal. Methods*. 9 (2016) 2701-2710.
- [21] M. Akhoundian, A. Ruter, S. Shinde, Ultratrace detection of histamine using a molecularly imprinted polymers based imprinted sensors, *Sensors*. 17 (2017) 645-653.
- [22] S. Carinelli, M. Martí, S. Alegret, M.I. Pividori, Biomarker detection of global infectious diseases based on magnetic particles, *New Biotechnol.* 32 (2015) 521-532 .
- [23] D. Brandão, S. Liébana, M.I. Pividori, Multiplexed detection of food borne pathogens based on magnetic particles, *New Biotechnol.* 32 (2015) 511-520.
- [24] R.T. Ma, Y.P. Shi, Magnetic molecularly imprinted polymer for the selective extraction of quercetagenin from *Calendula officinalis* extract, *Talanta*. 34 (2015) 650-656



- [25] Q.C. Zhang, X.H. Xio, G.K. Li, Porous molecularly imprinted monolithic capillary column for on-line extraction coupled to high-performance liquid chromatography for trace analysis of antimicrobials in food samples, *Talanta*. 123 (2014) 63-70.
- [26] R.J. Uzuriaga-Sánchez, S. Khan, A. Wong, G. Picasso, M.I. Pividori, M.D.P.T. Sotomayor, Magnetically separable polymer (Mag-MIP) for selective analysis of biotin in food samples, *Food chemistry* 190 (2016) 460-467.
- [27] Y. Guo, T.Y. Guo, A dual-template imprinted capsule with remarkably enhanced catalytic activity for pesticide degradation and elimination simultaneously, *Chem.Commun.* 49 (2013) 1073-1075.
- [28] A. Ben Aissa, A. Herrera-Chacon, R.R. Pupin, M.D.P.T. Sotomayor, M.I. Pividori, Magnetic molecularly imprinted polymer for the isolation and detection of biotin and biotinylated biomolecules, *Biosensors and Bioelectronics* 88 (2017) 101-108.
- [29] S.L. Moura, L.M. Fajardo, L. dos Anjos Cunha, MDPT Sotomayor, F.B.C. Machado, L.F.A. Ferrão, M.I. Pividori, Theoretical and experimental study for the biomimetic recognition of levothyroxine hormone on magnetic molecularly imprinted polymer, *Biosensors and Bioelectronics* 107 (2018) 203-210
- [30] A.H.A. Hassan, S.L. Moura, F.H.M. Ali, W.A. Moselhy, M.D.P.T., Sotomayor, M. I., Pividori, Electrochemical sensing of methyl parathion on magnetic molecularly imprinted polymer, *Biosens. Bioelectron* 118 (2018) 181–187.
- [31] M.I. Pividori, S. Alegret, Electrochemical genosensing based on rigid carbon composites. A review, *Analytical Letters* 38 (2005) 2541-2565
- [32] E. Zacco, M.I. Pividori, S. Alegret, R. Galvé, M.P. Marco, Electrochemical magnetoimmunosensing strategy for the detection of pesticides residues *Analytical chemistry* 78 (2006) 1780-1788

[33] A. Ben Aissa, J.J. Jara, R.M. Sebastián, A. Vallibera, S. Campoy, M.I. Pividori. Comparing nucleic acid lateral flow and electrochemical genosensing for the simultaneous detection of foodborne pathogens. *Biosensors and Bioelectronics* 88 (2017) 265-272.



## Graphical Abstract

### Highlights

- The synthesis of a novel hybrid magnetic molecularly imprinted (magnetic-MIP) with a great binding affinity and selectivity toward histamine
- The synthesized magnetic-MIP was integrated in magneto-actuated procedures based on the direct electrochemical detection of histamine
- This material succeeded in the preconcentration of histamine from scombroid fish
- The recovery rate ranged between 96.8- 102.0 %.